Equilibrium Thermodynamics of Pseudoelasticity and Quasiplasticity

Stefan Seelecke
Weierstraß-Institut
für Angewandte Analysis und Stochastik
im Forschungsverbund Berlin e.V.
Mohrenstraße 39
D-10117 Berlin

22.12.1995

Abstract

Motivated by recent experimental results by Glasauer [7], a thermodynamic theory of shape memory alloys is proposed, which includes not only the high temperature - pseudoelastic - behavior but also the low temperature range of quasiplasticity. Due to the occurance of three different phases - austenite and two martensitic variants - several cases of two-phase equilibria and a three-phase equilibrium have to be taken into account. Their relevance is determined by minimization of the total free energy and subsequently illustrated by the construction of phase charts. A special point of interest is the influence of interfacial energy effects on these phase charts, resulting in phenomena like, for example, the apparent violation of Gibbs' phase rule. Furthermore, their role in the hysteretic load-displacement behavior is discussed in the light of the additional quasiplastic case.

1 Introduction

Shape memory alloys show a strongly temperature dependent load-displacement behavior, termed *pseudoelastic* at elevated and *quasiplastic* at lower temperatures. A diversity of experimental and theoretical research results can be found, for example, in the various proceedings of the International Conference on Martensitic Transformations (ICOMAT) [16, 5, 19, 17, 15].

For a general overview of the behavior and different approaches to thermodynamic modeling of quasiplasticity and pseudoelasticity, see [13].

In both cases, one observes the occurance of hysteresis loops, connected with phase transitions in the underlying crystal structure. Due to its accessibility in a simple tensile experiment, the pseudoelastic hysteresis has been the subject of detailed investigations for some years now. For example, Xu [11] studied its temperature dependence in the case of *CuZnAl* single crystals, and in [6], Fu found a complex structure of load-deformation paths in the interior of the hysteresis. In a further experiment, he recorded the number of interfaces evolving during the phase transition [9]. These observations have been modeled by Huo and Müller in [6, 9] and [8], who developed a systematic thermodynamic theory of pseudoelasticity.

Only recently, Glasauer [7] performed experiments in the entire tension-compression range, which made it possible to study the complete quasiplastic hysteresis, including its internal structure. In [18], an extension of the existing thermodynamic theory of shape memory alloys is given to account for these new observations. The main ideas of this work are reviewed in the present paper.

For this purpose, the following section starts with a brief overview of the key aspects of Glasauer's results.

Section 3 then recalls the fundamental concept of equilibrium thermodynamics and provides the constitutive theory necessary to describe phase transitions. Equilibrium conditions are derived, which - in the context of deformation-controlled experiments - lead to the requirement for the total free energy of the specimen to attain a minimum.

This minimization is performed in the first part of section 4. In contrast to pseudoelasticity, the occurance of three phases - austenite and two martensitic variants - gives rise to several possible multi-phase configurations of the body. Their relevance is illustrated by the construction of phase charts, which resemble the temperature-composition phase diagrams of binary alloys. As in that case, they indicate the domain of control parameters - here temperature T and displacement D, where the corresponding configurations represent stable equilibrium states. In particular, the influence of interfacial energy on these phase charts is studied. For example, it allows for the existence of three-phase equilibria along line segments instead of confining them to a single point as predicted by the classical Gibbs' phase rule. Moreover, it leads to the observation that the phase deformations no longer coincide with phase boundaries as they do for vanishing interfacial energy. Finally, load-displacement diagrams are constructed, and the comparison of the pseudoelastic and quasiplastic hysteresis loops shows that interfacial energy cannot be the sole ingredient to hysteretic behavior.

2 Experimental Observations

In [7], Glasauer has studied the load-deformazion behavior of *CuZnAl* single crystals. With a specially designed device he was able to perform not only tensile experiments, but to enter the compressive range as well. This made it possible to record a complete quasiplastic hysteresis, including the paths in its interior. Fig. 1 shows several such paths, which are the result of unloading upon partial yield or reloading upon partial recovery. Even though

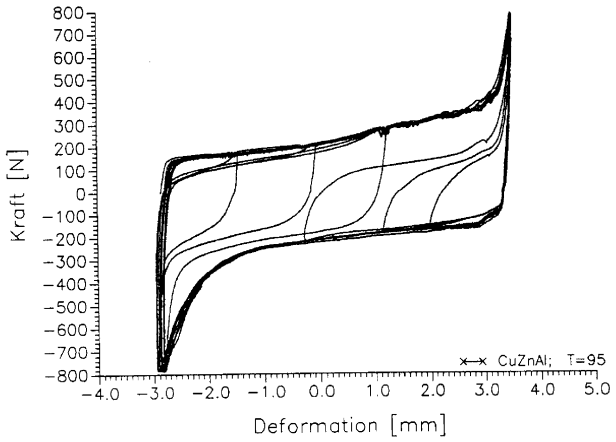

Figure 1: *Internal load-deformation paths of the quasiplastic hysteresis in a CuZnAl single crystal*

the behavior is not as pronounced as in the pseudoelastic case (see [6] for comparison), it shows very similar characteristics. For each internal path, there is a point that indicates the onset of internal yielding or recovery, respectively, and the connection of these points also produces a diagonal line like in the pseudoelastic case.

Fig. 2 - 4 show the results of complete tensile-compressive loading cycles at different temperatures. Fig. 2 depicts the pseudoelastic behavior at high temperatures with two hysteresis loops, fig. 4 shows the quasiplastic hysteresis, and fig. 3 is recorded at an intermediate temperature, showing the transition between the two extremes.

Observation of the specimen surface reveals that it is necessary to account for at least three phases. The tensile pseudoelastic hysteresis is connected with a load-induced transformation from austenite to a variant of martensite, oriented favorably to the direction of the applied load[1]. During the compres-

[1]For an introduction to the theory of martensitic transformations, see [2, 3, 4] and [20], for example.

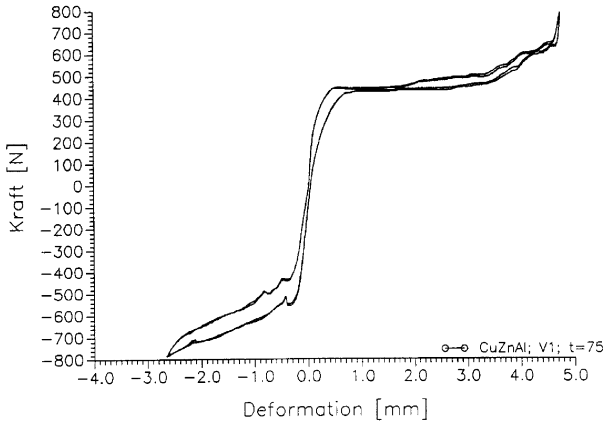

Figure 2: *Pseudoelastic behavior of a* CuZnAl *single crystal in tension and compression [7]*

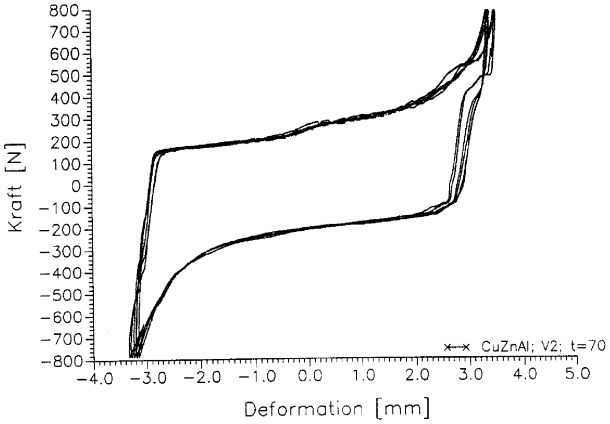

Figure 3: *Transition Pseudoelasticity⟷Quasiplasticity*

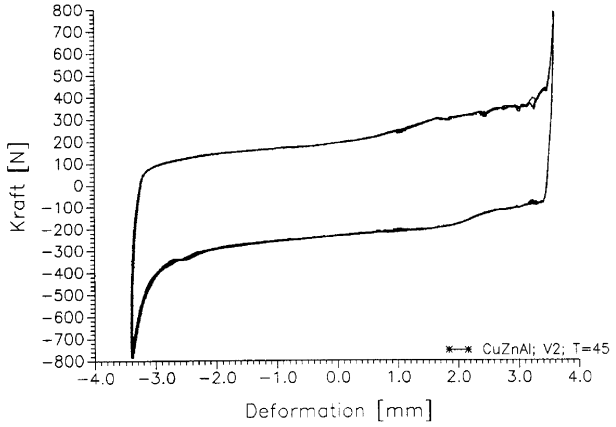

Figure 4: *Quasiplastic hysteresis loop [7]*

sive hysteresis, we observe the formation of a symmetry-related variant, which - under the reversed load - is now sheared to the opposite direction as in the tensile case. The quasiplastic hysteresis turns out to be the consequence of a transformation from one martensitic variant to the other.

Furthermore, it can be observed that all phase transitions proceed by the formation and annihilation of an immense number of alternating layers, thus causing a corresponding number of interfaces between the individual phases. In the pseudoelastic case, this phenomenon has been studied by Fu [9], who counted the number of these interfaces as a function of phase fraction, see fig. 5.

Finally, it is important to note that all reported experiments have been performed quasistatically. In addition to this, only negligibly small relaxation effects have been observed [14], so that we interpret the state in the material as a state of - at least metastable - thermodynamic equilibrium.

3 Equilibrium Thermodynamics

Application of the first and second law of thermodynamics to a one-dimensional tensile experiment yields the following thermodynamic stability criterion:

$$\frac{d}{dt}\left(U - T_0 S\right) \leqq -S\frac{dT_0}{dt} + P\frac{dD}{dt} \ . \tag{1}$$

U and S are internal energy and entropy of the body under consideration. D is the end displacement of the bar, P is the load necessary to maintain it and T_0 is the temperature at the surface of the specimen.

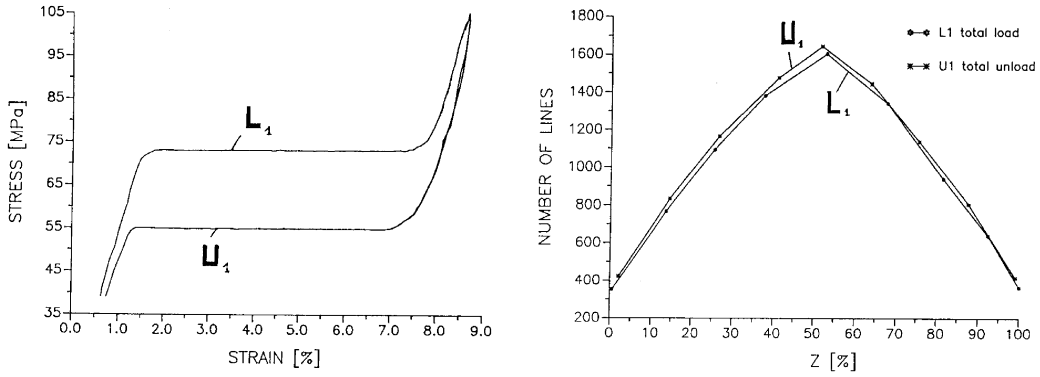

Figure 5: *Number of interfaces vs. phase fraction during a complete pseudoelastic hysteresis loop [9]*

Obviously, this criterion is useful if temperature and displacement are the quantities that are controlled in the experiment. In particular, if they are fixed, the combination $U - T_0 S$ decreases with time until it reaches a stationary value in equilibrium, where the equality sign in (1) is valid. This implies the equilibrium condition

$$U - T_0 S \quad \text{to be} \quad \textit{minimal.} \tag{2}$$

It is relevant in a quasistatic experiment, because here, experimental observation suggests that the adjustment of equilibrium is considerably faster than the change in displacement. Thus, the latter is seen by the body as a sequence of constant levels, under which it establishes a corresponding sequence of equilibria.

3.1 Availability

For further evaluation of (2), it is necessary to specify the availability $\mathcal{A}_D := U - T_0 S$, which - in the context of this paper - will be subject to the following assumptions:

1. The body is one-dimensional, in particular the displacement vector is of the form $u_i = (u_1(x), 0, 0)$.

2. The only phases occuring are the austenitic phase A and two martensitic phases M_+ and M_-. These are the oppositely sheared twins of the only variant observed in a uniaxial experiment. In the one-dimensional

picture, M_+ contributes to an elongation of the bar and M_- to its shortening.

3. The mass density ρ is assumed to be constant and equal for all three phases.

4. The contribution of an individual interface to the availability is given by

$$\sigma_{\Delta\Gamma} bh.$$

$\sigma_{\Delta\Gamma}$ is called interfacial energy coefficient between the phases Δ and Γ. It is a measurable quantity and - due to crystal symmetry - is the same for combinations A/M_+ and A/M_-. b and h are thickness and height of the bar, respectively.

Accounting for the fact that the phase transformation proceeds by the formation of alternating layers of different phases, we write the availability as sums over the individual layers and intermediate interfaces:

$$\frac{\mathcal{A}_D}{bh} = \sum_{\Gamma} \sum_{\alpha=1}^{N_\Gamma} \int_{l_\Gamma^\alpha}^{r_\Gamma^\alpha} \rho \left(u_\Gamma - T_0 s_\Gamma \right) dx + \sum_{\Delta \neq \Gamma} N_{\Delta\Gamma} \sigma_{\Delta\Gamma}, \qquad (3)$$

$$\text{with } \Gamma, \Delta \in [A, M_+, M_-] \,.$$

l_α^Γ and r_α^Γ are the left- and right-hand side coordinates of layer α in phase Γ. N_Γ denotes the total number of layers in this phase, and $N_{\Delta\Gamma}$ is the number of interfaces between Δ and Γ. To avoid lenghty notation, a summation over the three phases is introduced which is indicated by the subscript Γ, and the subscript $\Delta \neq \Gamma$ symbolizes that the corresponding summation is to be performed over all three possibilities of differing indices. Due to the constitutive quantities $u = u(\epsilon, T)$ and $s = s(\epsilon, T)$, $\mathcal{A}_D$ depends on the deformation field $\epsilon(x) := \partial u_1 / \partial x$ and the temperature field $T(x)$ as well as on the distribution of the phases, characterized here by $N_{\Delta\Gamma}, N_\Gamma$, l_α^Γ and r_α^Γ. It has to be minimized subject to the three constraints

$$L = \sum_{\Gamma} \sum_{\alpha=1}^{N_\Gamma} \int_{l_\Gamma^\alpha}^{r_\Gamma^\alpha} dx \,, \qquad (4)$$

$$D = \sum_{\Gamma} \sum_{\alpha=1}^{N_\Gamma} \int_{l_\Gamma^\alpha}^{r_\Gamma^\alpha} \epsilon(x)\, dx \qquad \text{and} \qquad (5)$$

$$0 = \sum_{\Gamma} N_\Gamma - 1 - \sum_{\Delta \neq \Gamma} N_{\Delta\Gamma}. \qquad (6)$$

The first condition expresses the fact that the phase arrangement has to take place under fixed length of the bar, while the second one gives the resulting end displacement D as the sum of integrals over the deformation field in each layer. The last condition connects the number of interfaces with the number of layers.

The constraints are incorporated into the functional by Lagrange multipliers so that the subsequent minimization can be performed without constraints on the expression

$$\begin{aligned} \mathcal{A}_D^* &= \mathcal{A}_D + \alpha \left(L - \sum_{\Gamma} \sum_{\alpha=1}^{N_\Gamma} \int_{l_\Gamma^\alpha}^{r_\Gamma^\alpha} dx \right) + \lambda \left(D - \sum_{\Gamma} \sum_{\alpha=1}^{N_\Gamma} \int_{l_\Gamma^\alpha}^{r_\Gamma^\alpha} \epsilon(x)\, dx \right) \\ &\quad + \gamma \left(\sum_{\Gamma} N_\Gamma - 1 - \sum_{\Delta \neq \Gamma} N_{\Delta\Gamma} \right). \end{aligned} \tag{7}$$

α, λ and γ are the Langrange multipliers mentioned above.

3.2 Equilibrium Conditions I

From (7) follows the necessary condition for equilibrium

$$\delta \mathcal{A}_D^* = 0\,, \tag{8}$$

which is evaluated in two steps. First, the variation with respect to the temperature field $T(x)$ and the deformation field $\epsilon(x)$ gives[2]

$$\left(\frac{\partial u_\Gamma}{\partial \epsilon} \right)_T - T_0 \left(\frac{\partial s_\Gamma}{\partial \epsilon} \right)_T - \frac{\lambda}{\rho b h} = 0 \qquad \text{and} \tag{9}$$

$$\left(\frac{\partial u_\Gamma}{\partial T} \right)_\epsilon - T_0 \left(\frac{\partial s_\Gamma}{\partial T} \right)_\epsilon = 0\,. \tag{10}$$

(9) and (10) represent three equations each, valid in every single layer of phase Γ.

Assuming local equilibrium, one can further exploit (9) and (10), using the Gibbs equation

$$T ds = du - \frac{\sigma}{\rho} d\epsilon\,, \tag{11}$$

where σ is the 11-component of the stress tensor. Its application yields the conditions for thermal and mechanical equilibrium

$$T(x) = T_0 \quad \text{and} \quad \sigma(x) = \frac{\lambda}{bh}\,, \tag{12}$$

[2]For a detailed discussion of the derivation, see **??**.

requiring temperature and stress to be constant throughout the bar. Moreover, if $(12)_2$ is applied to the end of the bar, λ can be identified as the load P.

The resulting deformation field, however, cannot be calculated without further knowledge of the constitutive functions $u_\Gamma(\epsilon, T)$ and $s_\Gamma(\epsilon, T)$, or - with $(12)_1$ - the free energy density $f_\Gamma(\epsilon, T)$. Additionally, the insertion of these quantities considerably simplifies the evaluation of the remaining conditions for phase equilibrium. For this reason, the following section derives an expression for the free energy density suitable for the description of phase transitions.

3.3 A Model Free Energy Density for Shape Memory Behavior

The calculation of the free energy density again relies on the local validity of the Gibbs equation. The simplest case is the one of a linearly elastic material without thermal expansion obeying a generalized Hooke's law:

$$\sigma_\Gamma = E(\epsilon_\Gamma - \epsilon_\Gamma^*). \tag{13}$$

Here, the Young's modulus E is the same for each phase and ϵ_Γ^* is the known stress-free transformation strain

$$\epsilon_\Gamma^* = \begin{cases} \epsilon^T & (\text{martensite } M_+) \\ 0 & (\text{austenite } A) \\ -\epsilon^T & (\text{martensite } M_-) \end{cases} . \tag{14}$$

If also the specific heat c is taken to be the same for each phase and independent of temperature, the Gibbs equation in the form

$$df_\Gamma = -s_\Gamma dT + \frac{\sigma_\Gamma}{\rho} d\epsilon \tag{15}$$

can be integrated to yield

$$f_\Gamma(\epsilon, T) = \Theta_\Gamma(T) + \frac{1}{2\rho} E(\epsilon - \epsilon_\Gamma^*)^2 \tag{16}$$

with

$$\Theta_\Gamma(T) = -cT \ln \frac{T}{T_R} + c(T - T_R) - s_\Gamma^R(T - T_R) . \tag{17}$$

Thus, the free energy is given by a parabolic dependence on strain, shifted along the ϵ-axis according to the phase under consideration. The functions $\Theta_\Gamma(T)$ must be such that martensite is stable at low temperatures and

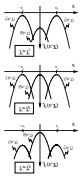

austenite at high temperatures. They are adjusted by a proper choice of the entropy constants s^R_Γ, which is the reason that this behavior is termed *entropic stabilization* of austenite. Note that, due to crystal symmetry, $s^R_+ = s^R_-$.

Figure 6 shows the free energy density for several different temperatures. The intermediate diagram, where all three minima are at the same height, refers to the case $T_2 = T_R$, the temperature of the reference state.

because of $T(x) = T_0$, has become the total free energy F, reading

$$\frac{F}{bh} = \sum_{\Gamma} \rho f_{\Gamma}(\epsilon_{\Gamma}, T) \sum_{\alpha=1}^{N_{\Gamma}} \int_{l_{\Gamma}^{\alpha}}^{r_{\Gamma}^{\alpha}} dx + \sum_{\Delta \neq \Gamma} N_{\Delta\Gamma} \sigma_{\Delta\Gamma} \,. \tag{18}$$

Note that thus the explicit dependence on $N_{\Gamma}, l_{\Gamma}^{\alpha}$ and r_{Γ}^{α} has vanished. Instead, upon introduction of specific quantitites, the phase distribution is solely given by the phase fractions

$$z_{\Gamma} := \frac{1}{L} \sum_{\alpha=1}^{N_{\Gamma}} \int_{l_{\Gamma}^{\alpha}}^{r_{\Gamma}^{\alpha}} dx \,, \tag{19}$$

and the specific free energy reads

$$f := \frac{F}{m} = \sum_{\Gamma} z_{\Gamma} f_{\Gamma}(\epsilon_{\Gamma}, T) + \sum_{\Delta \neq \Gamma} N_{\Delta\Gamma} \frac{\sigma_{\Delta\Gamma}}{\rho L} \,. \tag{20}$$

Insertion of the free energy density (16) also modifies the constraints to

$$1 = \sum_{\Gamma} z_{\Gamma} \quad \text{and} \tag{21}$$

$$\frac{D}{L} = \sum_{\Gamma} z_{\Gamma} \epsilon_{\Gamma} \,. \tag{22}$$

The third condition is rendered superflous, because N_{Γ} does not appear among the list of variables anymore.

A final remark has to be given with respect to the dependence on the number of interfaces $N_{\Delta\Gamma}$. According to the present model, the first sum in (20), representing the bulk contribution of the phases, depends only on the phase fraction regardless of the number of layers and thus the number of interfaces. Upon minimization of f with respect to $N_{\Delta\Gamma}$, this leads to the circumstance that the number of interfaces will always take on the values $N_{\Delta\Gamma} = 1$ if the phases Δ and Γ are present. As this is not in good agreement with experimental observations, $N_{\Delta\Gamma}$ are dropped from the list of variables and rather interpreted as constitutive quantities, for which an ansatz of the form

$$N_{\Delta\Gamma} = C_{\Delta\Gamma} z_{\Delta} z_{\Gamma} \qquad \text{(no summation)} \tag{23}$$

is made. This goes back to a proposition originally made by Müller [10]. It links the number of interfaces to the phase fraction in such a way that they are zero for the case of pure phase Δ or Γ, respectively, and run through a

maximum inbetween. This corresponds to the results of figure 5, which also allow for the determination of the proportionality coefficients $C_{\Delta\Gamma}$.

As a conclusion of the foregoing results, the possible equilibrium states of a shape memory bar are obtained from the minimization of the following augmented free energy function

$$\begin{aligned} f^* &= \sum_{\Gamma} z_\Gamma f_\Gamma\left(\epsilon_\Gamma, T\right) + \sum_{\Delta\neq\Gamma} C_{\Delta\Gamma} z_\Delta z_\Gamma \frac{\sigma_{\Delta\Gamma}}{\rho L} + \alpha\left(1-\sum_{\Gamma} z_\Gamma\right) \\ &\quad + \lambda\left(\frac{D}{L}-\sum_{\Gamma} z_\Gamma \epsilon_\Gamma\right). \end{aligned} \tag{24}$$

4 Equilibrium States

For the subsequent treatment, it is useful to introduce the dimensionless quantities

$$\begin{aligned} \tilde{\epsilon}_\Gamma &:= \frac{\epsilon_\Gamma}{\epsilon^T}, \\ \tilde{D} &:= \frac{D}{L\epsilon^T} \qquad \text{and} \end{aligned} \tag{25}$$

$$\tilde{f} := \frac{f}{\frac{E}{\rho}\left(\epsilon^T\right)^2} = \sum_{\Gamma} z_\Gamma \tilde{f}_\Gamma \quad \text{with} \quad \tilde{f}_\Gamma := \tilde{\Theta}_\Gamma\left(\tilde{T}\right) + \tfrac{1}{2}\left(\tilde{\epsilon}_\Gamma - \tilde{\epsilon}^*_\Gamma\right)^2 \quad , \tag{26}$$

$$\text{where} \qquad \tilde{\epsilon}^*_\Gamma := \begin{cases} 1 & (\text{martensite } M_+) \\ 0 & (\text{austenite } A) \\ -1 & (\text{martensite } M_-) \end{cases} . \tag{27}$$

$A_{\Delta\Gamma}$ denote the dimensionless interfacial energy coefficients with

$$A_{\Delta\Gamma} := \frac{\sigma_{\Delta\Gamma} C_{\Delta\Gamma}}{EL\left(\epsilon^T\right)^2}, \tag{28}$$

and the augmented free energy reads

$$\tilde{f}^* := \sum_{\Gamma} z_\Gamma \tilde{f}_\Gamma + \sum_{\Delta\neq\Gamma} A_{\Delta\Gamma} z_\Delta z_\Gamma + \tilde{\alpha}\left(1-\sum_{\Gamma} z_\Gamma\right) + \tilde{\lambda}\left(\tilde{D}-\sum_{\Gamma} z_\Gamma \epsilon_\Gamma\right), \tag{29}$$

with $\tilde{\alpha}$ and $\tilde{\lambda}$ being the dimensionless Lagrange multipliers

$$\begin{aligned} \tilde{\lambda} &:= \frac{\lambda}{E\epsilon^T bh} \qquad \text{and} \\ \tilde{\alpha} &:= \frac{\alpha}{E\left(\epsilon^T\right)^2}. \end{aligned} \tag{30}$$

4.1 Necessary Conditions for Equilibrium

The resulting necessary conditions for equilibrium read

$$
\begin{aligned}
0 &= \left(\frac{\partial \tilde{f}_A}{\partial \tilde{\epsilon}_A}\right)_T - \tilde{\lambda} = \tilde{\epsilon}_A - \tilde{\lambda}\,, \\
0 &= \left(\frac{\partial \tilde{f}_+}{\partial \tilde{\epsilon}_+}\right)_T - \tilde{\lambda} = (\tilde{\epsilon}_+ - 1) - \tilde{\lambda}\,, \\
0 &= \left(\frac{\partial \tilde{f}_-}{\partial \tilde{\epsilon}_-}\right)_T - \tilde{\lambda} = (\tilde{\epsilon}_- + 1) - \tilde{\lambda}\,, \\
0 &= \left(\frac{\partial \tilde{f}^*}{\partial z_A}\right)_{T,\epsilon_\Gamma,z_\Gamma \neq z_A} = \tilde{f}_A - \tilde{\alpha} - \tilde{\lambda}\tilde{\epsilon}_A + A_{AM}\,(z_+ + z_-)\,, \qquad (31) \\
0 &= \left(\frac{\partial \tilde{f}^*}{\partial z_+}\right)_{T,\epsilon_\Gamma,z_\Gamma \neq z_+} = \tilde{f}_+ - \tilde{\alpha} - \tilde{\lambda}\epsilon_+ + A_{AM} z_A + A_{+-} z_-\,, \\
0 &= \left(\frac{\partial \tilde{f}^*}{\partial z_-}\right)_{T,\epsilon_\Gamma,z_\Gamma \neq z_-} = \tilde{f}_- - \tilde{\alpha} - \tilde{\lambda}\epsilon_- + A_{AM} z_A + A_{+-} z_+\,, \\
1 &= z_A + z_+ + z_- \qquad \text{and} \\
\tilde{D} &= z_A\tilde{\epsilon}_A + z_+\tilde{\epsilon}_+ + z_-\tilde{\epsilon}_-\,.
\end{aligned}
$$

In $(31)_{1,2,3}$, the first three equations represent the conditions for mechanical equilibrium, while $(31)_{4,5,6}$ is the one-dimensional form of those for phase equilibrium. Together with the last two equations - representing the constraints - (31) is a system for the determination of the unknown deformation in each phase, its phase fraction and the two Lagrange multipliers. Note that thermal equilibrium is already taken into account by replacing the availability by the free energy.

So far, the entire treatment assumed equilibrium among all three phases. Even though this is the general case, there are also the cases of two-phase equilibrium or single-phase existence, which need to be taken into account. Altogether, there are seven different configurations for the body, which will be discussed in a systematic manner as special cases of the general system (31).

4.1.1 Single-phase existence

Austenite A: The martensite phase fractions are identically zero, $z_+ = z_- = 0$, and the relevant equations for the evaluation are $(31)_{1,4,7,8}$. From $(31)_7$, it follows

$$z_A = 1 \tag{32}$$

[3]and, from $(31)_8$,

$$\epsilon_A = D \, . \tag{33}$$

With $(31)_1$, one concludes

$$\lambda = D \, , \tag{34}$$

and due to $(31)_4$, it is possible to identify

$$\alpha = f_A - \sigma \epsilon_A = g_A \tag{35}$$

as the free enthalpy. The free energy f finally reads

$$f = f_A \left(\epsilon_A, T \right) = \frac{1}{2} D^2 + \Theta_A \left(T \right) = f \left(D, T \right) \, . \tag{36}$$

Martensite M_+ or M_-: In this case, the following phase fractions vanish, $z_A = z_- = 0$ or $z_A = z_+ = 0$, respectively. The evaluation relies on $(31)_{2,5,7,8}$ or $(31)_{3,6,7,8}$. In analogy to the previous case, $(31)_7$ yields

$$z_\pm = 1 \, , \tag{37}$$

and $(31)_8$ gives

$$\epsilon_\pm = D \, . \tag{38}$$

From $(31)_2$, it follows

$$\lambda = D \mp 1 \, , \tag{39}$$

and due to $(31)_5$, it is again possible to identify

$$\alpha = f_\pm - \sigma \epsilon_\pm = g_\pm \, . \tag{40}$$

The upper sign is valid for the case "M_+" and the lower one for "M_-". As before, the free energy f depends on D and T, reading

$$f = f_\pm \left(\epsilon_\pm, T \right) = \frac{1}{2} \left(D \mp 1 \right)^2 + \Theta_M \left(T \right) = f \left(D, T \right) \, . \tag{41}$$

[3]For readability's sake, the tildes have been omitted again so that from here on all quantities are understood to be dimensionless.

4.1.2 Two-phase Coexistence

$\underline{M_+ \textbf{ and } M_-\textbf{:}}$ Here, the austenite phase fraction vanishes, $z_A = 0$, and $(31)_{2,3,5,6,7,8}$ are the relevant equations for this case. From $(31)_{2,3}$, one deducts

$$\epsilon_+ - \epsilon_- = 2, \tag{42}$$

from which follows, together with $(31)_5$ - $(31)_6$ and $(31)_{7,8}$,

$$\lambda = \frac{1}{2} A_{+-} \left(1 - D + \epsilon_-\right) \ . \tag{43}$$

The phase deformation as well as the Lagrange multiplier λ are determined by (43) and $(31)_{2,3}$ to give

$$\epsilon_+ = 1 - \frac{\frac{1}{2}A_{+-}}{1 - \frac{1}{2}A_{+-}} D \ , \tag{44}$$

$$\epsilon_- = -1 - \frac{\frac{1}{2}A_{+-}}{1 - \frac{1}{2}A_{+-}} D \qquad \text{and} \tag{45}$$

$$\lambda = -\frac{\frac{1}{2}A_{+-}}{1 - \frac{1}{2}A_{+-}} D \ . \tag{46}$$

From $(31)_{7,8}$, the phase fractions can be calculated,

$$z_+ = \frac{D - \epsilon_-}{\epsilon_+ - \epsilon_-} = \frac{1}{2}\left(1 + \frac{D}{1 - \frac{1}{2}A_{+-}}\right) \qquad \text{as well as} \tag{47}$$

$$z_- = \frac{\epsilon_+ - D}{\epsilon_+ - \epsilon_-} = \frac{1}{2}\left(1 - \frac{D}{1 - \frac{1}{2}A_{+-}}\right) \ , \tag{48}$$

and from $(31)_{5,6}$, one obtains the other Lagrange multiplier

$$\alpha = g_+ + A_{+-} z_+ = g_- + A_{+-} z_- \ . \tag{49}$$

Finally, the free energy of the mixture reads

$$\begin{aligned} f &= z_+ f_+ \left(\epsilon, T\right) + z_- f_- \left(\epsilon, T\right) + A_{+-} z_+ z_- = \\ &= \frac{1}{2}\left(\epsilon_- + 1\right)^2 + \Theta_M \left(T\right) + A_{+-} z_+ \left(1 - z_+\right) \ . \end{aligned} \tag{50}$$

Range of admissibility: From the condition

$$0 < z_+ < 1 \, ,$$

it follows with $A_{+-} < 2$ that this case is only admissible , when - independent of temperature T - the control parameter D is in the range

$$-1 + \frac{1}{2}A_{+-} < D < 1 - \frac{1}{2}A_{+-} \ . \tag{51}$$

A and M_+ or A and M_-: This case is characterized by $z_- = 0$ or $z_+ = 0$, and the relevant equations are $(31)_{1,2,4,5,7,8}$ or $(31)_{1,3,4,6,7,8}$, respectively. From $(31)_{1,2}$ or $(31)_{1,3}$, one calculates the relation between the phase deformations

$$\epsilon_A - \epsilon_\pm = \mp 1 \,, \tag{52}$$

and with $(31)_4$ - $(31)_{5,6}$ and $(31)_{7,8}$ it is possible to identify λ as

$$\lambda = \frac{\pm B\left(T\right) \pm A_{AM}\left(1 \mp 2D\right)}{1 - 2A_{AM}} \tag{53}$$

with

$$B\left(T\right) := \Theta_M\left(T\right) - \Theta_A\left(T\right) \,. \tag{54}$$

Again, the upper sign is valid for "M_+" and the lower one for "M_-". $(31)_{1,2,3}$ then yield the phase deformations

$$\epsilon_A = \frac{\pm B\left(T\right) \pm A_{AM}\left(1 \mp 2D\right)}{1 - 2A_{AM}} \qquad \text{and} \tag{55}$$

$$\epsilon_\pm = \pm 1 + \frac{\pm B\left(T\right) \pm A_{AM}\left(1 \mp 2D\right)}{1 - 2A_{AM}} \tag{56}$$

as well as - due to $(31)_{7,8}$ - the phase fractions

$$z_A = \frac{\epsilon_\pm - D}{\epsilon_\pm - \epsilon_A} = 1 - \frac{\pm D - B\left(T\right) - A_{AM}}{1 - 2A_{AM}} \quad \text{and} \tag{57}$$

$$z_\pm = \frac{D - \epsilon_A}{\epsilon_\pm - \epsilon_A} = \frac{\pm D - B\left(T\right) - A_{AM}}{1 - 2A_{AM}} \,. \tag{58}$$

$(31)_{5,6}$ serve to compute the Lagrange multiplier α:

$$\alpha = g_A + A_{AM} z_\pm = g_\pm + A_{AM} z_A \,. \tag{59}$$

Finally, the free energy follows as

$$\begin{aligned} f &= z_A f_A\left(\epsilon, T\right) + z_\pm f_\pm\left(\epsilon, T\right) + A_{AM} z_A z_\pm = \\ &= f_A\left(\epsilon, T\right) + z_\pm\left[f_\pm\left(\epsilon, T\right) - f_A\left(\epsilon, T\right)\right] + A_{AM} z_A z_\pm = \\ &= \frac{1}{2}\epsilon_A^2 + \Theta_A\left(T\right) + z_\pm\left[B\left(T\right) + A_{AM}\left(1 - z_\pm\right)\right] \,. \end{aligned} \tag{60}$$

Range of admissibility: The admissibility of this case is limited to

$$\begin{aligned} B\left(T\right) &< D < 1 + B\left(T\right) - A_{AM} \qquad \text{for } A/M_+ \text{ or} \\ -1 - B\left(T\right) + A_{AM} &< D < -B\left(T\right) - A_{AM} \qquad \text{for } A/M_- \,, \end{aligned} \tag{61}$$

assuming $A_{AM} < 1/2$.

4.1.3 Three-phase Coexistence

The evaluation of the three-phase case requires all eight equations. $(31)_{1,2,3}$ give

$$\epsilon_A = \epsilon_+ - 1 = \epsilon_- + 1 \; . \tag{62}$$

and from $(31)_5$ - $(31)_6$, it follows

$$\lambda = -\frac{1}{2} A_{+-} \left(z_+ - z_- \right) \; , \tag{63}$$

or - together with $(31)_1$ and $(31)_{7,8}$ -

$$\lambda = -\frac{\frac{1}{2} A_{+-}}{1 - \frac{1}{2} A_{+-}} D \; . \tag{64}$$

The phase deformations are calculated from $(31)_{1,2,3}$ to be

$$\begin{aligned} \epsilon_A &= -\frac{\frac{1}{2} A_{+-}}{1 - \frac{1}{2} A_{+-}} D \; , \\ \epsilon_+ &= 1 - \frac{\frac{1}{2} A_{+-}}{1 - \frac{1}{2} A_{+-}} D \qquad \text{and} \\ \epsilon_- &= -1 + \frac{\frac{1}{2} A_{+-}}{1 - \frac{1}{2} A_{+-}} D \; , \end{aligned} \tag{65}$$

and from $(31)_{4,5,6}$, one obtains

$$\alpha = g_A + A_{AM} \left(z_+ + z_- \right) = g_+ + A_{AM} z_A + A_{+-} z_- = g_- + A_{AM} z_A + A_{+-} z_+ \; . \tag{66}$$

The phase fractions z_A, z_+ and z_- are determined from $(31)_4$ - $(31)_5$, $(31)_5$ - $(31)_6$ and $(31)_{7,8}$:

$$z_+ = \frac{1}{2} \left[\frac{B\left(T\right) + A_{AM}}{2A_{AM} - \frac{1}{2} A_{+-}} + \frac{1}{1 - \frac{1}{2} A_{+-}} D \right] \; , \tag{67}$$

$$z_- = \frac{1}{2} \left[\frac{B\left(T\right) + A_{AM}}{2A_{AM} - \frac{1}{2} A_{+-}} - \frac{1}{1 - \frac{1}{2} A_{+-}} D \right] \qquad \text{and} \tag{68}$$

$$z_A = 1 - \frac{B\left(T\right) + A_{AM}}{2A_{AM} - \frac{1}{2} A_{+-}} \; . \tag{69}$$

Insertion into the free energy finally gives

$$f = z_A f_A + z_+ f_+ + z_- f_- + A_{AM} z_A \left(z_+ + z_- \right) + A_{+-} z_+ z_- =$$

$$
\begin{aligned}
&= f_A + z_+ \left[f_+ - f_A\right] + z_- \left[f_- - f_A\right] + \\
&\quad + A_{AM} \left(1 - z_+ - z_-\right) \left(z_+ + z_-\right) + A_{+-} z_+ z_- \\
&= \frac{1}{2}\epsilon_A^2 + \Theta_A\left(T\right) + \left(z_+ + z_-\right) \left[B\left(T\right) + A_{AM}\left(1 - z_+ - z_-\right)\right] + \\
&\quad + A_{+-} z_+ z_- \ . \qquad (70)
\end{aligned}
$$

Range of admissibility: With $A_{AM} > A_{+-}/4$, the equation for z_A (69) restricts the admissible temperatures to

$$
-A_{AM} < B\left(T\right) < A_{AM} - \frac{1}{2} A_{+-} \ . \qquad (71)
$$

This, together with $z_+ > 0$ und $z_- > 0$, then limits the end displacement D to the range:

$$
-\left[B\left(T\right) + A_{AM}\right] \frac{1 - \frac{1}{2}A_{+-}}{2A_{AM} - \frac{1}{2}A_{+-}} < D < \left[B\left(T\right) + A_{AM}\right] \frac{1 - \frac{1}{2}A_{+-}}{2A_{AM} - \frac{1}{2}A_{+-}} \ . \qquad (72)
$$

From the previous results, the values of ϵ_Γ, z_Γ, α and λ are known for each of the seven cases. However, they follow from the necessary conditions only, and the question remains, which of the possible configurations is the one prevailing in equilibrium.

4.2 Sufficient Conditions for Equilibrium

To answer this question, it is necessary to determine the configuration which - for a given set of control parameters (D, T) - actually minimizes the free energy. In the case of vanishing interfacial energy, illustrative methods are provided by the well-known Maxwell construction and the common tangent construction. Unfortunately, these constructions are no longer applicable in the general case. The tangents to the free energy at the points ϵ_Γ are not equal to the slope of the line given by the difference quotient anymore. Instead, they differ from each other by an amount that depends on the actual value of D, which renders the method impracticable. To circumvent this inconvenience, a variant of the Maxwell construction has been employed by Müller and Bornert [1] for the treatment of the pseudoelastic phase transition. However, this method involves a cumbersome measuring of areas, and moreover, the Maxwell construction does not provide any evidence on the minimality characteristic of the considered case. As the latter is not a problem in pseudoelasticity, it is crucial for cases with more than two possible phases involved.

For this reason, the present paper follows a different path. With the knowledge of the individual free energies from the previous section, it is possible to *calculate* the transition points from one solution to another. Graphical methods are only employed in order to illustrate the behavior.

Figures 7 - 10 show plots of the seven total free energies[4] as functions of the end displacement D for several characteristic temperatures, represented by the function $B(T) := \Theta_M(T) - \Theta_A(T)$. The solid lines denote the single phases, while the phase mixtures can be identified by the following table:

$\cdots\cdots$	$A/M_+/M_-$
$-\cdot-\cdot-$	$A/M_\pm$
$---$	M_+/M_-

.

The underlying values for the interfacial energy coefficients are $A_{AM} = 0.1$ and $A_{+-} = 1/10 A_{AM} = 0.01$.[5] Their ratio reflects the fact that the interfacial energy arises because of a misfit at the phase boundaries. Due to the differing lattice parameters between austenite and martensite, the misfit of such a combination is considerably larger than the one of two martensite variants.

construction - they are given by straight lines, the free energies of the phase mixtures here are concave parabolae. Nevertheless, for $-1 + A_{+-}/2 < D < 1 - A_{+-}/2$, the mixture M_+/M_- represents the stable equilibrium, minimizing the total free energy in this range.

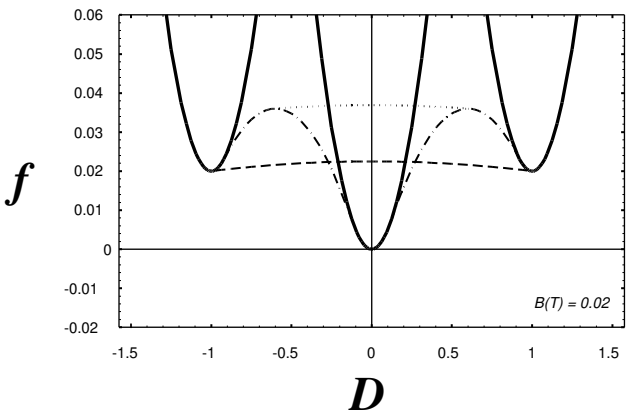
0.06
0.05
0.04
0.03
0.02
0.01
0
-0.01
-0.02
f
-1.5
-1
-0.5
0
0.5
1
1.5
D
B(T) = 0.02

small intermediate range of $|D|$, the body forms a mixture A/M_+ or A/M_-, respectively. However, with increasing end displacement and thus inreasing number of interfaces forming, this becomes unfavorable again compared to the case M_+/M_-.

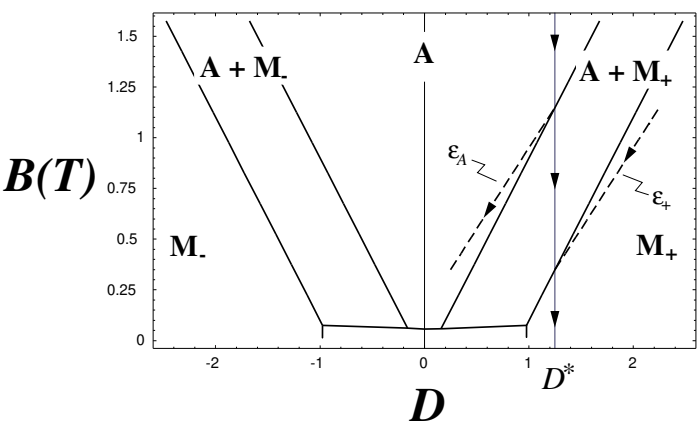
B(T)
1.5
1.25
1
0.75
0.5
0.25
0
-2
-1
0
1
2
D*
D
A + M-
A
A + M+
εA
ε+
M-
M+

interfacial energy where these quantities mark the onset of the phase transition, here, they do not coincide with the phase boundaries. This feature, too, makes it necessary to evaluate the sufficient conditions for equilibrium in order to construct a phase diagram. In the case without interfacial energy, the phase boundaries could be determined from the knowledge of the phase deformations following from the necessary conditions alone.

4.4 Load-displacement Diagrams

With the knowledge of the stable equilibrium configurations of the shape memory bar, it is possible to generate load-displacement diagrams that can be compared to experimental data. The load P had been identified as the Lagrange multiplier λ from (12) and is shown in figures 15 and 16 as function of D for temperatures corresponding to quasiplastic and pseudoelastic behavior.

ideas of Müller [11], one can deduct the size of the hysteresis from it. For the pseudoelastic case, he showed that this is determined by the coefficient of interfacial energy. If the interfacial energy is neglected in the treatment, the diagonal line becomes horizontal, which corresponds to a totally reversible phase transition without hysteresis.

for an interpretation of some characteristics of the hysteresis like size and internal diagonal line. Transferring these ideas to the present case, the latter remains valid, but the former points to a problem now. The identical lattice parameters had motivated a smaller interfacial energy for a combination of two martensitic variants than for one of austenite and martensite. Consequently, this should lead to a smaller hysteresis in the quasiplastic case. Experimental observations, however, show that it is approximately of the same order of magnitude as in the pseudoelastic case, a circumstance that points to yet another mechanism responsible for hysteretic behavior.

Acknowledgements

I express my thanks to Prof. I. Müller who initiated and communicated this work and to Prof. J. Sprekels for his support during the "production phase" of the paper.

References

[1] Bornert, M., Müller, I. (1990): Temperature dependence of hysteresis in pseudo-elasticity. In: *Free Boundary Value Problems* (Hoffmann, K.-H., Sprekels, J. (eds.)), 27 - 35. ISNM Vol. **95**. Basel, Birkhäuser Verlag

[2] Christian, J.W. (1970), Martensitic Transformations, in: *Physical Metallurgy*, R.W. Cahn (ed.), North-Holland, 552-587

[3] Christian, J.W. (1975), *Theory of Transformations in Metals and Alloys — Part I: Equilibrium and General Kinetic Theory*, Pergamon Press, 12-14

[4] Cohen, M., Wayman, C.M. (1981), Fundamentals of Martensitic Reactions, in: *Metallurgical Treatises*, Tien,J.K., Elliott, J.F. (eds.), The Metallurgical Society of AIME, Warrendale, PA, 455-468

[5] Delaey, L., Chandrasekharan, L. (eds.) (1982): *Proc. Int. Conf. on Martensitic Transformation, Leuven (Belgium). Journal de Physique* **43**.

[6] Fu, S., Huo, Y., Müller, I. (1993), Thermodynamics of Pseudoelasticity - An Analytical Approach, *Acta Mechanica,* **99**, 1-19

[7] Glasauer, F.U., Thermodynamische Untersuchungen an Gedächtnislegierungen, *Dissertation, TU Berlin*, in Vorbereitung

[8] Huo, Y., Müller, I. (1993), Non-equilibrium Thermodynamics of Pseudoelasticity, *Cont. Mech. Thermodyn.* **5,** 1-19

[9] Huo, Y., Müller, I. (1993), Thermodynamics of Pseudoelasticity - An Graphical Approach, In: Models of Hysteresis, Visintin, A. (ed.), *Pitman Research Notes in Mathematics* **286**, 39-58

[10] Müller, I. (1986), Pseudoelasticity in shape memory alloys – an extreme case of thermoelasticity. *Acad. Naz. Lincei. Proc. of the Meeting on Finite Thermoelasticity* **76**, 123 - 150

[11] Müller, I. (1989): On the size of hysteresis in pseudo-elasticity, *Cont. Mech. Thermodyn.* **1**, 125 - 142

[12] Müller, I., Xu, H. (1991): On the pseudo-elastic hysteresis, *Acta Metall.* **39**, 263 - 271

[13] Müller, I., Huo, Y., Seelecke, S. (1994): Quasiplasticity and Pseudoelasicity, *CIME Lecture Notes*, Heidelberg: Springer-Verlag

[14] Müller, I. (1995), Thermodynamics of Ideal Pseudoelasticity, *Journal de Physique* **IV**, Colloque C2, supplément au *J. Phys.* **III**, Volume 5, 423-431

[15] Ortin, J. (ed.) (1995): *Proc. Int. Conf. on Martensitic Transformation, Barcelona (Spain). Journal de Physique* **4**.

[16] Perkins, J. (ed.) (1976): *Shape Memory Effects in Alloys*. New York: Plenum Press.

[17] Perkins, J. (ed.) (1992): *Proc. Int. Conf. on Martensitic Transformation,* Monterey (USA).

[18] Seelecke, S. (1995), Zur Thermodynamik von Formgedächtnislegierungen, *Dissertation, TU Berlin*

[19] Tamura, I. (ed.) (1986): *Proc. Int. Conf. on Martensitic Transformation, Nara (Japan).* The Japan Institute of Metals

[20] Wayman, C.M. (1964), Introduction to the Crystallography of Martensitic Transformations, *MacMillan Series in Materials Science*